Available online at www.sciencedirect.com
ScienceDirect
Ceramics International 37 (2011) 3011–3018
CERAMICS INTERNATIONAL
www.elsevier.com/locate/ceramint

Synthesis and thermal properties of inorganic polymers (geopolymers) for structural and refractory applications from volcanic ash

Patrick N. Lemougna [a,b,c], Kenneth J.D. MacKenzie [b,*], U.F. Chinje Melo [a,c]

[a] Local Materials Promotion Authority, MINRESI/MIPROMALO, Yaounde, Cameroon
[b] MacDiarmid Institute for Advanced Materials and Nanotechnology, School of Chemical and Physical Sciences, Victoria University of Wellington, New Zealand
[c] Physico-Chemistry of Mineral Materials Laboratory, University of Yaoundé I, Cameroon

Received 7 February 2011; received in revised form 3 May 2011; accepted 3 May 2011
Available online 11 May 2011

Abstract

The volcanic ash occurring as an abundant and readily accessible natural resource in the Central African country of Cameroon was used to synthesize aluminosilicate geopolymers using sodium hydroxide as the sole alkaline activator. Both the curing conditions and the Na_2O/SiO_2 molar ratio were found to influence the development of compressive strength of the geopolymer cement paste, which achieved a maximum strength of 55 MPa at $Na_2O/SiO_2 = 0.3$. The formation of a mortar by the addition of 40 wt% sand to the optimized geopolymer cement composition reduced the compressive strength to 30 MPa, still within the useful range for construction applications. The geopolymers consist largely of X-ray amorphous material with a small content of crystalline phases. Scanning electron microscopy showed a homogenously distributed mixture of lath-shaped and agglomerated morphologies, with a homogeneous distribution of Si, Al and O in the geopolymer matrix. The geopolymers are relatively stable to heat, shrinking only slowly and retaining about 60% of their as synthesized compressive strength on heating to 900 °C. The FTIR spectra of both the as synthesized and heated geopolymers show two broad absorbance bands, between 820–1250 cm^{-1} and 450–730 cm^{-1} assigned to the internal vibrations of Si–O–Si, and Si–O–Al respectively. The compressive strengths and the thermal stability of these materials suggest their suitability for building applications and low-grade refractories.

Keywords: C. Mechanical properties; C. Thermal properties; D. Silicate; E. Structural applications

1. Introduction

Ordinary Portland cement (OPC) concrete is one of the most universal building materials [1,2], its production and use having greatly increased during the last decades especially in emerging and developing countries [3]. Although this material has excellent structural performances, its production generates CO_2 [4] accounting for up to 5% of anthropogenic emissions of this greenhouse gas [2].

Alternative low-energy materials such as inorganic polymers (geopolymers) produced from natural minerals or inorganic wastes have attracted interest in the last three decades as possible more ecologically friendly cementitious materials [4–7]. Geopolymers consist of tetrahedral aluminate and silicate units linked by oxygen atoms, the negative charge of Al^{3+} in IV-fold coordination being compensated by ions such as Na^+, K^+, and Li^+ [3–5]. The silicate and aluminate units are randomly distributed in the structure in a range of Si environments, generally with a predominance of $SiQ^4(2Al)$ and $SiQ^4(3Al)$ [5,7].

Since these materials cure and harden at ambient temperatures, their synthesis requires less energy, with about 80% less CO_2 production than for OPC [2,8]. A further advantage of these materials over OPC is their thermal stability; geopolymers synthesized from dehydrated kaolinite (metakaolin) or fly ash are reported to be relatively stable up to 800–1200 °C, with only a small degree of shrinkage and good strength retention [7,9,10], whereas the mechanical properties of OPC are seriously degraded above 400 °C [4,9].

Theoretically, any pozzolanic mineral or source of silica and alumina that is readily soluble in alkali may serve as a geopolymer precursor [1,3]. However, most of the studies to

* Corresponding author. Tel.: +64 4 462 5885; fax: +64 4 463 5237.
E-mail address: Kenneth.mackenzie@vuw.ac.nz (K.J.D. MacKenzie).

0272-8842/$36.00 © 2011 Published by Elsevier Ltd and Techna Group S.r.l.
doi:10.1016/j.ceramint.2011.05.002

date have focused on metakaolin and fly ash raw materials [7–16], with very few reports on volcanic ash-based geopolymers despite the relative abundance of this aluminosilicate material in countries with past or present volcanism [17–19]. These minerals, which are deposited at the surface during volcanic activity are readily accessible and have the advantage that they can be economically mined, with enormous benefits of low cost and limited negative environmental impact compared with traditional open pit quarry-type clay mining [17].

Furthermore, the possibility of obtaining geopolymers from such aluminosilicate sources without the need for the thermal activation required for 1:1 clay minerals should present an additional advantage in terms of low energy consumption. One country in which abundant resources of such volcanic ash are available is Cameroon, in Central Africa. The successful development of geopolymer building materials and low-grade refractories would be of significant economic benefit to Cameroon, and to other countries with similar volcanic ash deposits.

The aim of this study was to investigate the synthesis, structure and properties of geopolymers from Cameroonian volcanic ash. The structure of the polymers was studied by XRD and FTIR and the influence of the molar composition and curing conditions on the compressive strength of the geopolymer cement was determined, as were the mechanical and physical properties of the corresponding mortar containing various proportions of standard mortar sand. The thermal properties of these materials were also determined by TGA/DSC and dilatometry, to assess their suitability as refractories.

2. Experimental

2.1. Materials

The volcanic ash used in this study was from the Foumbot Petponoun site, Cameroon. The material was ground to pass a 400 μm sieve. The resulting particle size distribution, determined using a Shimadzu Sald-2001 Laser diffraction particle size analyzer, is shown in Fig. 1. The aggregate used to prepare the mortar samples was New Zealand natural sand with a density of 2.56 g/cm^3 and size distribution (Fig. 1) determined according to ASTM C 778-00. The chemical composition of the volcanic ash and sand aggregate as determined by X-ray fluorescence is presented in Table 1.

2.2. Geopolymer synthesis

The inorganic polymers were synthesized by stirring the volcanic ash into a solution of NaOH (Applichem Co.) in distilled water, to give five compositions with Na_2O/SiO_2 molar ratios of 0.15–0.35. The weight ratio (H_2O:volcanic ash) was maintained at 0.21 in all the formulations. The mixed paste was stirred for 5 min, placed in 50 mm × 50 mm × 50 mm cubic polythene moulds and vibrated for 5 min to remove air bubbles.

One of the mixtures ($Na_2O/SiO_2 = 0.25$) was subjected to various curing procedures as follows: 40 °C for 24 h sealed, then unsealed at 40 °C for 24 h. This initial curing was the same for all the samples, and was followed by post-curing for five days, either in water or in the open air at 40, 70 and 90 °C. The post-curing environment that produced the best compressive strength (dry curing at 90 °C) was then adopted for the remaining experiments.

Mortars were produced by adding 10, 25 and 40 wt% of sand in the basis of the volcanic ash, to the cement paste formulation with the best compressive strength.

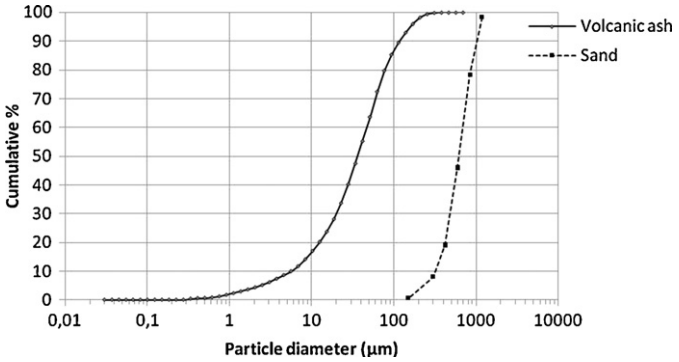

Fig. 1. Particle size distributions of the volcanic ash and mortar sand used in this work.

2.3. Sample characterization

The compressive strengths of the samples cured for 7 days were measured using an ELE ADR-Auto 2000 kN compression tester with the force applied at a rate of 0.9 kN/s. The results are reported as the average for three replicates.

The broken samples were powdered and examined by X-ray diffraction (Philips PW1700 with a computer-controlled goniometer and graphite monochromator with Co Kα radiation). The powdered samples were also pressed into KBr pellets for FTIR analysis using a Perkin Elmer FTIR spectrometer.

EDS maps and scanning electron micrographs were determined in the backscattered mode on fractured samples coated with 16 nm of carbon using a Jeol JSM 6500F microscope operated at 15.0 kV.

Water absorption and bulk density were measured on sectioned samples by the Archimedes principle. The density and open porosity values were determined as the average of three samples of each composition.

Table 1
Chemical composition of volcanic ash and mortar sand.

Oxide	Fe_2O_3	MnO	TiO_2	CaO	K_2O	P_2O_5	SiO_2	Al_2O_3	MgO	Na_2O	LOI	SUM
Volcanic ash	13.22	0.18	2.74	10.38	1.53	0.61	44.19	14.06	9.73	3.69	−0.62	99.71
Sand	3.22	0.10	0.27	3.98	1.33	0.08	68.54	15.93	1.04	4.30	0.93	99.71

The thermal behavior of the sample of composition $Na_2O/SiO_2 = 0.25$ dry-cured at 90 °C was determined by differential scanning calorimetry (DSC) and thermogravimetry (TG) using a TA instruments SDT Q600 V8.2 in flowing air (50 ml/min) and a heating rate of 10 °C min^{-1}.

The dilatometric curve was obtained on a cylindrical sample 20.15 mm × 6 mm dia. using a modified Harrop Laboratories TDA-H1-CP6 dilatometer at a heating rate of 5 °C min^{-1} up to 1000 °C, held at this temperature for 0.5 h then cooled at 5 °C min^{-1} to about 100 °C. The sample was subjected to two cycles.

Samples of composition $Na_2O/SiO_2 = 0.25$ were heated in a Carbolite 3216 electric kiln to 250 °C, 500 °C, 750 °C, 900 °C and 1000 °C at a heating rate of 5 °C min^{-1} and a dwell time of 2 h at each temperature followed by natural cooling in the kiln. The compressive strengths of these specimens were then measured.

3. Results and discussion

3.1. Effect of processing conditions on the mechanical properties and structure of geopolymer pastes

Although all the sample formulations developed strength after curing period, the strength of the sample with $Na_2O/SiO_2 = 0.15$ was too low to be determined by the compressive test machine, probably due to insufficient reaction in this composition. This confirms the trends observed by Duxson et al. [16], who suggested that the presence of a significant amount of unreacted material in the geopolymer matrix increases the defect density of the specimens, decreasing the mechanical strength. All the dry-cured samples showed some efflorescence, particularly in the sample with $Na_2O/SiO_2 = 0.35$, which also displayed major cracking.

The seven-day compressive strengths of the sample of composition $Na_2O/SiO_2 = 0.25$ subjected to various curing conditions are shown in Fig. 2. The compressive strength increases significantly as the curing temperature is increased from 40 to 90 °C, the samples post-cured in water (wet) showing consistently lower compressive strengths, unlike the behavior of conventional cementitious products. The trends observed in the compressive strength values (14–42 MPa and 23–49 MPa for wet and dry post-curing respectively) are similar to those reported for flyash/clay geopolymers by van Jaarsveld et al. [20] who observed a substantial improvement of compressive strength when the curing temperature was increased from 30 to 70 °C. Wet curing of volcanic ash-based geopolymer may have the effect of removing the unreacted sodium species, counteracting the formation of efflorescence in the final products.

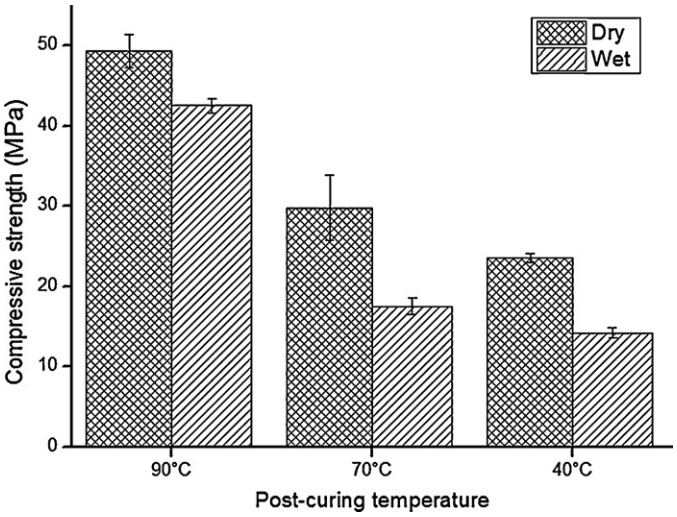

Fig. 2. Effect of post-curing temperature under wet and dry conditions on the 7-day compressive strength of geopolymers of molar composition $Na_2O/SiO_2 = 0.25$.

The 7-day compressive strengths of all the samples subjected to dry post-curing at 90 °C are presented in Fig. 3 which shows that the strength reaches a maximum at the composition $Na_2O/SiO_2 = 0.3$ before decreasing again at $Na_2O/SiO_2 = 0.35$. The observed values (13–55 MPa) are similar to those obtained by Duxson et al. [14] from metakaolin-based geopolymers containing Na and/or K as the alkali cation, within the Si/Al composition range 1.15–1.4. These results indicate that sufficient alkali must be present for complete dissolution of the starting materials, giving an increased geopolymerisation rate and higher compressive strength. A similar dependence of the geopolymerisation reaction on the sodium hydroxide concentration was also reported by Temuujin et al. [21] who observed a reduction in compressive strength when additional water was used in the synthesis. The degradation of strength at the highest Na_2O/SiO_2 molar ratio is probably due to the formation of significant efflorescence and crack formation. These observations are consistent with those obtained by Rüscher et al. [15] who reported that the coexistence of an aluminosilicate network and silicate chains in the correct proportion and spatial distribution maximizes the mechanical strength of the geopolymer matrix; excess NaOH was therefore suggested to cause weakening of the structure, favoring network formation while destroying the polymeric silicate chains.

The open porosities and bulk densities of the samples of all compositions are presented in Table 2. The sample of

Table 2
Water absorption and bulk density of the geopolymer paste and mortar samples.

Sample	Paste	Paste	Paste	Paste	Mortar, 10% sand	Mortar, 25% sand	Mortar, 40% sand
Na_2O/SiO_2 molar ratio	0.20	0.25	0.30	0.35	0.30	0.30	0.30
Water absorption (%)	16.95 (0.40)	14.08 (0.28)	14.24 (0.73)	14.80 (0.37)	14.61 (0.71)	12.55 (0.13)	11.34 (0.10)
Bulk density (g cm^{-3})	1.86 (0.03)	1.91 (0.03)	1.91 (0.02)	1.86 (0.03)	1.91 (0.02)	1.92 (0.02)	1.97 (0.02)

Figures in parentheses are the standard deviation of three measurements.

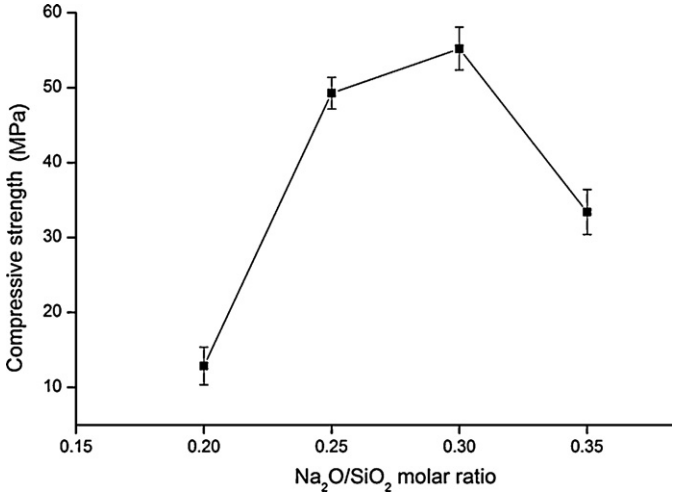

Fig. 3. Influence of the Na_2O/SiO_2 oxide molar ratio on the 7-day compressive strength of geopolymers post-cured at 90 °C under dry conditions.

composition $Na_2O/SiO_2 = 0.2$ showed the lowest density and the highest water absorption, probably because it contains less of the reaction product than in the other compositions. The water absorption values are all <15%, apart those of the sample with $Na_2O/SiO_2 = 0.2$, satisfying the requirement of these products for building applications according to ASTM standards C216 (SW).

The X-ray patterns of both the volcanic ash and resulting geopolymers (Fig. 4) show a large amount of amorphous material, in addition to the crystalline minerals augite/diopside ($Ca(Mg,Fe,Al)(Si,Al)_2O_6$, PDF no. 41-1483), ordered anorthite ($(Ca, Na)(Al,Si)_2Si_2O_8$, PDF no. 20-528) and ferroan forsterite ($(Mg,Fe)_2SiO_4$, PDF no. 31-795). The intensities of some of the crystalline diffraction peaks are reduced in the geopolymer paste, possibly due to the formation of additional amorphous phase and the appearance of the new phase $Na_8(AlSiO_4)_6(OH)_2{\cdot}4H_2O$ (PDF no. 41-9) resulting from the reaction of the volcanic ash with NaOH. Although conventional geopolymers are X-ray amorphous [12,13,22–24], the presence of crystalline phases in geopolymers prepared from volcanic ash has previously been reported [18,19]. By treating an amorphous pozzolan with sodium hydroxide or sodium hydroxide plus sodium aluminate, Verdolotti et al. [19] obtained a product with crystalline diffraction peaks, possibly from a zeolite, overlapping the amorphous baseline.

Since the initial volcanic ash contains calcium, iron and magnesium, these elements may have taken part in the formation of the geopolymer structure, either by integrating in the network or acting as crystalline fillers. Previous studies [25,26] reported the presence of calcium in the geopolymer raw material improves the mechanical properties due to the possible reduction of microstructural porosity resulting from the formation of amorphous Ca–Al–Si gel. The influence of different calcium compounds on metakaolin-based geopolymers [27] showed XRD features of conventional geopolymer composites containing additional crystalline fillers, suggesting that calcium may either act as filler, or integrate with the geopolymer network, depending on the chemical form of the

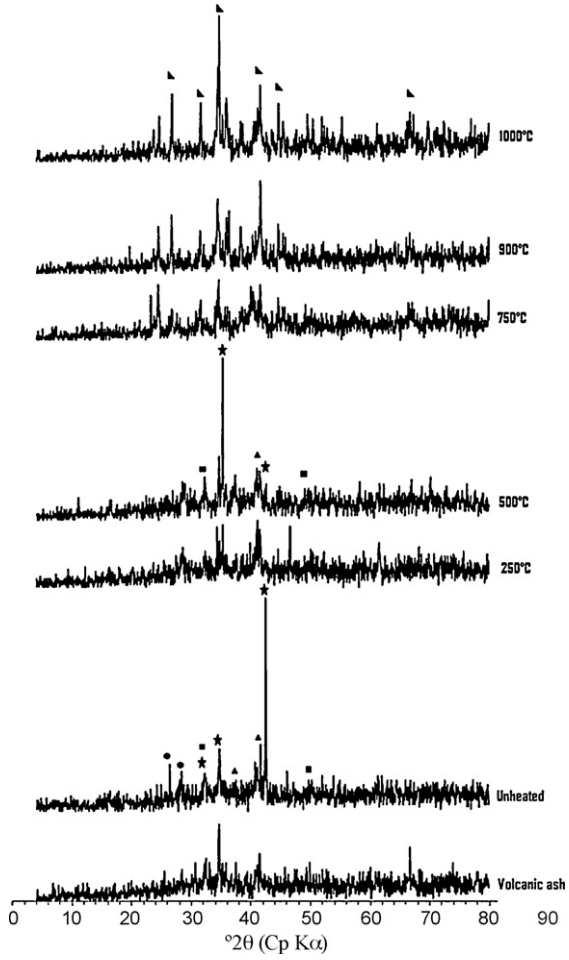

Fig. 4. X-ray powder diffraction patterns of the volcanic ash starting material and resulting geopolymers of molar composition $Na_2O/SiO_2 = 0.25$, unheated and thermally treated at the indicated temperatures. Key: ●—sodium aluminum silicate hydroxide hydrate, $Na_8(AlSiO_4)_6(OH)_2{\cdot}4H_2O$ (PDF no. 41-9); ★—alumimian augite, $Ca(Mg, Fe, Al)(Si,Al)_2O_6$ (PDF no. 41-1483); ■—sodium anorthite, $(Ca, Na)(Al,Si)_2 Si_2O_8$ (PDF no. 20-528); ▲—ferroan forsterite, $(Mg,Fe)_2SiO_4$ (PDF no. 31-795); ◣—nepheline, $(Na,K)AlSiO_4$ (PDF no. 1-89-8763).

additive. The behavior of magnesium and iron may be similar to that of calcium. Iron has been suggested possibly to be detrimental to geopolymer network formation by removing OH^-, thereby slowing down the dissolution of residual aluminosilicate [28], but this is at variance with Perera et al. [29], who reported that iron resides in octahedral sites in metakaolin-based geopolymers, either as isolated ions in the geopolymer matrix or as oxyhydroxide aggregates which had not reacted with the starting geopolymer components. Thus, in the present geopolymers, some of the ferrous iron remains in the various microcrystalline phases present in the original volcanic ash, but may also occupy specific geopolymer sites instead of forming $Fe(OH)_2$, imparting a homogeneous color to the samples, and a homogeneous iron distribution, as revealed by EDS maps (not shown here).

SEM/EDS examination of the fractured surface of the sample with $Na_2O/SiO_2 = 0.25$ showed a more or less

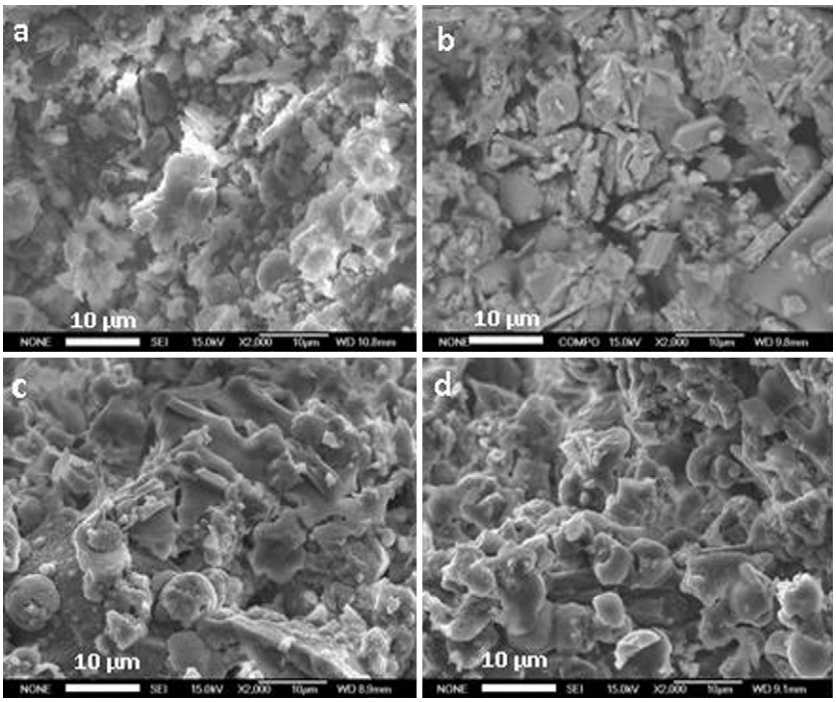

Fig. 5. SEM microstructure of geopolymer of molar composition $Na_2O/SiO_2 = 0.25$ (a) as-synthesized, (b) heated at 500 °C, (c) heated at 750 °C, and (d) heated at 900 °C.

homogeneous distribution of Si, Al, Fe, Na, Ca and O in the geopolymer matrix.

Areas of high Si concentration were associated with high Al concentration, indicating the presence of undissolved aluminosilicate particles in the geopolymer matrix. Mg was less homogeneously distributed in the matrix, suggesting that this element probably does not participate in the geopolymer formation reaction. Higher magnification revealed a mixture of lath-shaped and agglomerated morphologies (Fig. 5) which persisted in samples heated up to 900 °C (Fig. 5d). However, above 750 °C, a slight increase in the lath lengths is seen, possibly due to the onset of some solid state reactions.

The FTIR spectra of the initial volcanic ash and resulting geopolymers, both unheated and heated to various temperatures (Fig. 6) show two broad absorbance bands, at 820–1250 cm^{-1} and 450–730 cm^{-1} assigned to the internal vibrations of Si–O–Si and Si–O–Al respectively.

The main difference between the spectra of the initial volcanic ash and the NaOH-activated geopolymer is a shoulder at about 1500 cm^{-1} arising from sodium carbonate. The bands at 1700 cm^{-1} and 3500 cm^{-1} arise from the presence of structural water remaining in the geopolymer matrix after dry post-curing at 90 °C. The FTIR spectra of the volcanic ash and resulting geopolymer are very similar to those reported by Verdolotti et al. [19] in materials synthesized from Italian pozzolans with sodium hydroxide and sodium aluminate. These authors suggest that the broadness of the absorbance band at 820–1250 cm^{-1} reflects the variability of the bond angles and bond lengths of the tetrahedral structures around the silicon atoms, and the absorbance peak at 730 cm^{-1} arises from the stretching vibration of AlVI–O–Si bonds. The coordination of

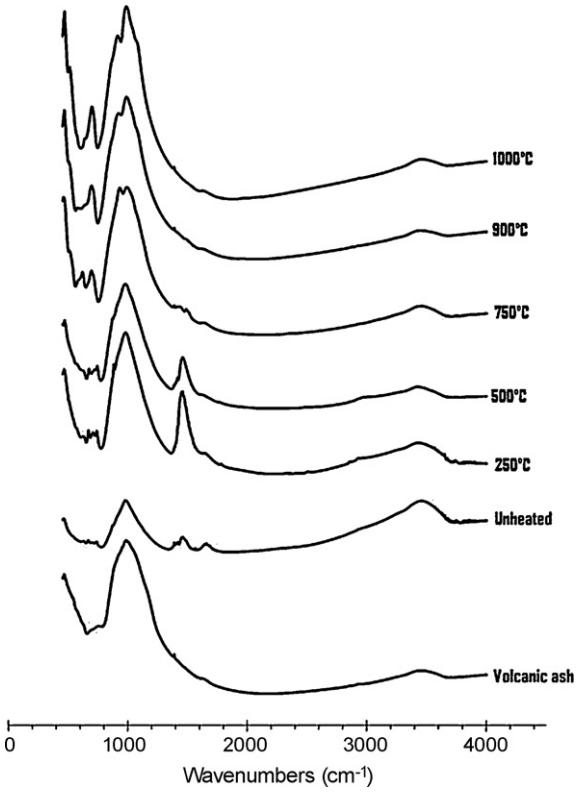

Fig. 6. FTIR spectra of the initial volcanic ash and geopolymer sample of molar composition $Na_2O/SiO_2 = 0.25$, unheated and thermally treated at the indicated temperatures.

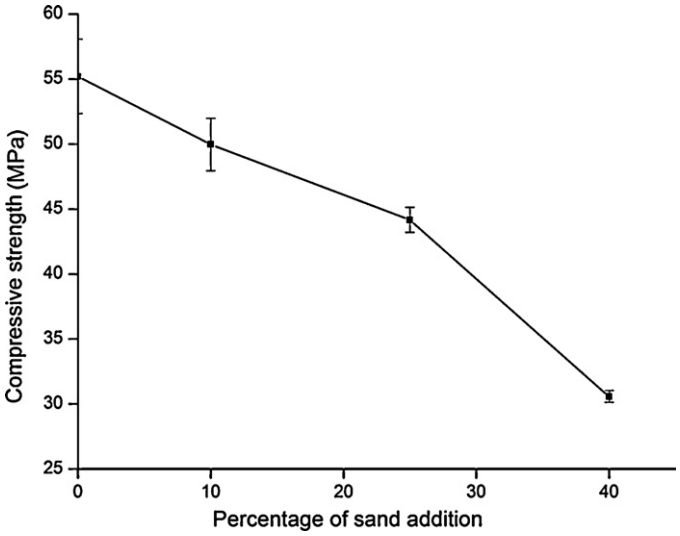

Fig. 7. Influence of the addition of mortar sand on the compressive strength of a mortar of molar composition $Na_2O/SiO_2 = 0.3$.

Al and Si in the present geopolymers could not be confirmed by solid-state MAS NMR spectroscopy because of the content of iron present.

3.2. Properties of mortar from geopolymer paste

The effect of adding varying amounts of mortar sand to the geopolymer paste of composition $Na_2O/SiO_2 = 0.3$ is shown in Fig. 7. Although the addition of sand reduces the porosity and increases the bulk density of the geopolymer mortar, the resulting compressive strength is less than for the geopolymer matrix, and decreases as the proportion of sand increases. This strength decrease may be the result of diluting the geopolymer by the sand without contributing any significant strength of its own. These results are similar to those obtained for a metakaolin-based geopolymer by Barbosa and MacKenzie [7] who reported a reduction of compressive strength upon adding 10–20 vol.% of various granular inorganic fillers. By contrast, different behaviors were reported in fly ash-based geopolymer [30], in which no significant change in strength was obtained by the addition of up to 50% sand, suggesting a partial dissolution of the aggregate surface in the geopolymer matrix giving increased interfacial bonding. Thus, the present volcanic ash geopolymer more closely resembles the behavior of metakaolin-based geopolymer than flyash geopolymer. Strength development of geopolymer mortars may therefore vary from case to case depending on the strength of the geopolymer gel, the interfacial bonding between the geopolymeric gel, the aggregate itself [30] and even the aggregate particle size distribution. In any case, the addition of sand filler can reduce manufacturing costs provided it is not added in proportions greater than required to maintain the physical properties appropriate to the proposed application. The compressive strength of 30 MPa obtained with 40% sand addition is still within the requirements of ASTM C216 (SW) for building materials.

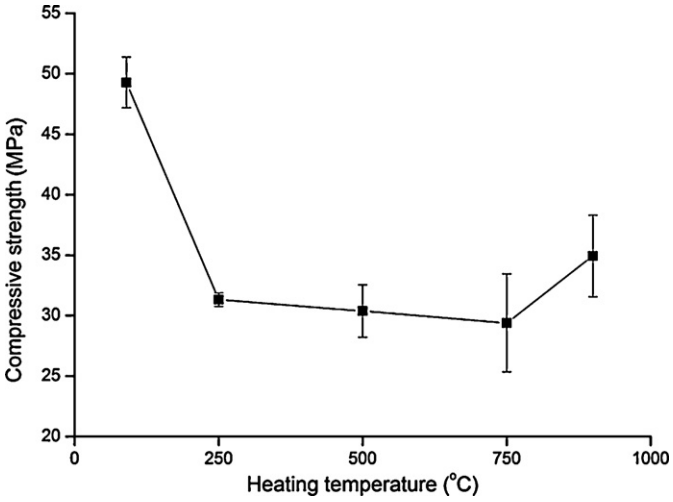

Fig. 8. Effect of thermal treatment temperature on the compressive strength of a geopolymer paste of molar composition $Na_2O/SiO_2 = 0.25$.

3.3. Effect of heat on the geopolymer products

The effect on the compressive strength of heating the sample with $Na_2O/SiO_2 = 0.25$ to various temperatures is shown in Fig. 8. Heating to 250 °C results in a significant strength reduction to 30 MPa, which is then maintained to 750 °C. Above this temperature the strength increases to about 35 MPa at 900 °C. The reduction of strength upon initial heating is probably due to the loss of structural water from the geopolymer matrix, weakening the structure, and also to the possible concomitant development of micro cracks.

The DSC/TG curves of the sample with $Na_2O/SiO_2 = 0.25$ (Fig. 9) show about 70% of the mass loss occurs <250 °C; this is attributed to the loss of structural water, since the negligible loss on ignition value for this volcanic ash indicates the absence of organic matter. The mass loss at about 250–600 °C is attributed to the removal of more tightly bound water and probably also reflects the decomposition at 400 °C of sodium carbonate formed by atmospheric carbonation of unreacted NaOH. Above 900 °C, the DSC curve shows an exothermic

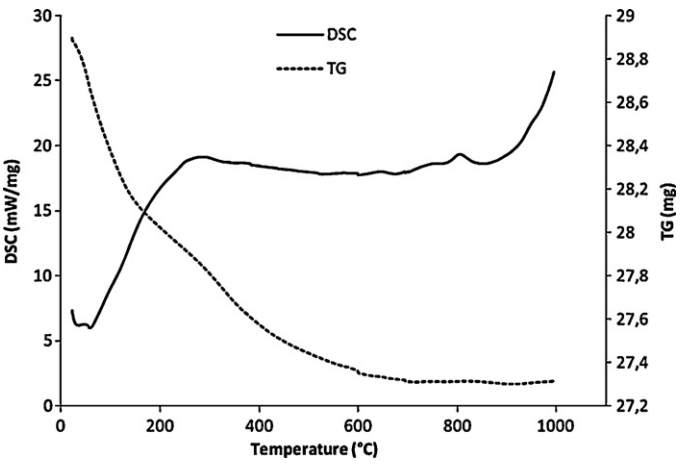

Fig. 9. DSC/TG curves of a geopolymer paste of molar composition $Na_2O/SiO_2 = 0.25$.

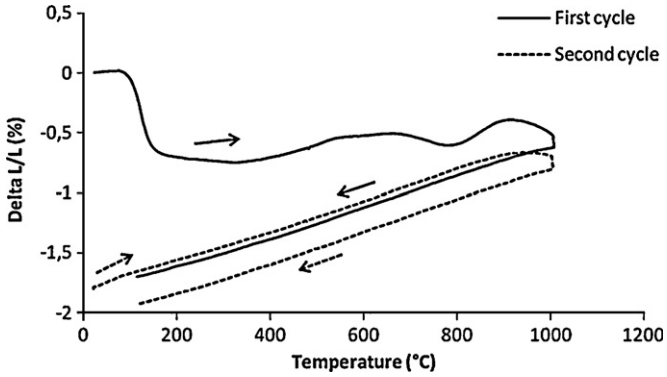

Fig. 10. Dilatometer curves of a geopolymer paste of molar composition $Na_2O/SiO_2 = 0.25$.

reaction, due to the formation of new phases with a concomitant onset of sintering of the geopolymer matrix. Similar behavior was observed in the sample shrinkage during the first heating cycle (Fig. 10). Between room temperature and about 110 °C, the 0.4% linear shrinkage is due to the removal of less tightly bound water as the drying process is completed.

Above this temperature the sample dimensions remain relatively constant up to 1000 °C. Over the last hundred degree the sample continued to shrink, reflecting a small degree of sintering.

During the cooling cycle the fired material shrank more or less linearly with a coefficient of thermal expansion of about $12 \times 10^{-6}\ C^{-1}$. The overall shrinkage of the sample after firing to 1000 °C and cooling is 1.8%, confirmed by measuring with calipers before and after firing.

During the second heating cycle, the sample expanded linearly only up to about 900 °C before starting to shrink between this temperature and 1000 °C (Fig. 10). Cooling produced a coefficient of thermal expansion similar to the first heating cycle and permanent shrinkage occurs only >900 °C. Thus, when the sample cools below 900 °C, permanent shrinkage stops and the remaining change of length is due to the recovery of the thermal expansion. The overall shrinkage after heating and cooling during the second cycle was about 0.25%.

The physical evolution of materials during heating is a critical factor in determining their suitability for applications ranging from construction to refractories and adhesives [31].

Compared to the overall shrinkage value of about 8% observed by Barbosa and MacKenzie [7] or Duxson et al. [31] for metakaolin-based geopolymer heated to 800–900 °C, the shrinkage of the present volcanic ash-based geopolymer is about four times smaller, indicating a superior dimensional stability within this temperature range.

The FTIR spectra (Fig. 6) show that there is no major phase transformation upon heating to 500 °C, apart from the removal of structural water and possibly the migration of unreacted Na compounds due to thermal activation. Above 750 °C there is no further evidence of sodium carbonate, which begins to decompose at 400 °C. The appearance at 750 °C of a new shoulder at about 1015 cm^{-1} is due to the formation of a new phase, the intensity of which increases with increasing temperature.

Similarly, the XRD diffractograms of the heated samples (Fig. 4) indicate no major phase transformation up to 500 °C. Apart from the destruction of the sodium aluminum silicate hydroxide hydrate by the removal of structural water at 110 °C, the major new crystalline phase formed is nepheline ($(Na,K)AlSiO_4$, PDF no. 1-89-8763); this nepheline appears at about 750 °C and is clearly observable by XRD at 900 °C. The oxidation of ferrous iron upon heating is also likely, in view of the color change from grey to brown in samples heated at 750–1000 °C. These high-temperature iron phases could not be identified by XRD because of their relatively small concentration. Neither can solid-state reactions leading to amorphous or glassy phases be ruled out, and are likely in view of the increase in the intensity of the amorphous characteristics of the X-ray traces at higher temperatures.

Taking into account the thermal analysis results and the thermal evolution of the microstructure, phase transformation becomes significant only >900 °C. This may reflect the geological origin of the volcanic ash, and its previous high temperature thermal history.

A deeper understanding of geopolymer formation from volcanic ash would repay further investigation because of the complexity of the starting material. Although the iron content in the present raw material militated against study by solid state nuclear magnetic resonance, a Mossbauer spectroscopic study of role played by the iron would be of interest.

4. Conclusions

Volcanic ash was used to produce inorganic polymers (geopolymers), using sodium hydroxide as the sole alkaline activator. The results show that this low-energy geopolymerisation process can synthesize this natural pozzolanic starting material into viable products with properties suitable for building and low-grade refractories applications.

Both the curing conditions (temperature, wet or dry conditions) and the Na_2O/SiO_2 molar ratio were found to influence the development of the compressive strength. Dry curing gave a product with a superior compressive strength (about 50 MPa) compared to the same material cured in water. The optimum compressive strength in this material (about 55 MPa) was obtained for samples with $Na_2O/SiO_2 = 0.30$, but higher Na_2O concentrations were found to be detrimental to the mechanical properties. The addition of sand to produce a mortar reduced the compressive strength, but the resulting samples were still within the ASTM recommendations for building materials.

The geopolymer products were found to be relatively stable to heat, retaining about 60% of their initial compressive strength and shrinking only slowly up to 900 °C. The compressive strengths of the heated materials and their thermal behavior suggest their suitability as low-grade refractories as well as in potential building applications.

Acknowledgements

We are indebted to David Flynn for assistance with the electron microscopy, Martin Ryan for assistance with the X-ray diffraction, Neville Baxter for the particle size analysis and thermal analysis, Andrew Durant for advice on the compressive strength testing and general discussions. This work was supported by funding from the Local Materials Promotion Authority, Cameroon (to PNL) and the MacDiarmid Institute for Advanced Materials and Nanotechnology.

References

[1] D. Khale, R. Chaudhary, Mechanism of geopolymerization and factors influencing its development: a review, J. Mater. Sci. 42 (2007) 729–746.
[2] J. Tailby, K.J.D. MacKenzie, Structure and mechanical properties of aluminosilicate geopolymer composites with Portland cement and its constituent minerals, Cem. Concr. Res. 40 (2010) 787–794.
[3] J. Davidovits, Geopolymer Chemistry and Applications, second edition, Institut Géopolymère, Paris, 2008.
[4] J. Davidovits, Geopolymers: inorganic polymeric new materials, J. Therm. Anal. 37 (1991) 1633–1656.
[5] S.J. O'Connor, K.J.D. MacKenzie, Synthesis, characterisation and thermal behaviour of lithium aluminosilicate inorganic polymers, J. Mater. Sci. 45 (2010) 3707–3713.
[6] K.J.D. MacKenzie, N. Rahner, M.E. Smith, A. Wong, Calcium-containing inorganic polymers as potential bioactive materials, J. Mater. Sci. 45 (2010) 999–1007.
[7] V.F.F. Barbosa, K.J.D. MacKenzie, Thermal behaviour of inorganic geopolymers and composites derived from sodium polysialate, Mater. Res. Bull. 38 (2003) 319–331.
[8] M. Izquierdo, X. Querol, J. Davidovits, D. Antenucci, H. Nugteren, C. Fernandez-Pereira, Coal fly ash-slag-based geopolymers: microstructure and metal leaching, J. Hazard. Mater. 166 (2009) 561–566.
[9] L.Y. Kong, S. Daniel, G.J. Sanjayan, Effect of elevated temperatures on geopolymer paste, mortar and concrete, Cem. Concr. Res. 40 (2010) 334–339.
[10] W.T. Cheng, P.J. Chiu, Fire-resistant geopolymer produced by granulated blast furnace slag, Miner. Eng. 16 (2003) 205–210.
[11] J.L. Bell, P.E. Driemeyer, W.M. Kriven, Formation of ceramics from metakaolin-based. Geopolymers: Part I—Cs-based geopolymer, J. Am. Ceram. Soc. 92 (2009) 1–8.
[12] H. Rahier, B. Van Mele, M. Biesemans, J. Wastiels, X. Wu, Low-temperature synthesized aluminosilicate glasses. Part I. Low-temperature stoichiometry and structure of a model compound, J. Mater. Sci. 31 (1996) 71–79.
[13] J.L. Bell, P.E. Driemeyer, W.M. Kriven, Formation of ceramics from metakaolin-based geopolymers. Part II. K-based geopolymer, J. Am. Ceram. Soc. 92 (2009) 607–615.
[14] P. Duxson, S.W. Mallicoat, G.C. Lukey, W.M. Kriven, J.S.J. van Deventer, The effect of alkali and Si/Al ratio on the development of mechanical properties of metakaolin-based geopolymers, Colloids Surf. A: Physicochem. Eng. Aspects 292 (2007) 8–20.
[15] C.H. Rüscher, E. Mielcarek, W. Lutz, A. Ritzmann, W.M. Kriven, Weakening of alkali-activated metakaolin during aging investigated by the molybdate method and infrared absorption spectroscopy, J. Am. Ceram. Soc. 93 (2010) 2585–2590.
[16] P. Duxson, J.L. Provis, G.C. Lukey, S.W. Mallicoat, W.M. Kriven, J.S.J. van Deventer, Understanding the relationship between geopolymer composition, microstructure and mechanical properties, Colloids Surf. A: Physicochem. Eng. Aspects 269 (2005) 47–58.
[17] C. Leonelli, E. Kamseu, D.N. Boccaccini, U.C. Melo, A. Rizzuti, N. Billong, P. Misselli, Volcanic ash as alternative raw materials for traditional vitrified ceramic products, Adv. Appl. Ceram. 106 (2007) 1.
[18] E. Kamseu, C. Leonelli, D.S. Perera, U.C. Melo, P.N. Lemougna, Investigation of volcanic ash-based geopolymers as potential building materials, Interceram 58 (2009) 136–140.
[19] L. Verdolotti, S. Iannace, M. Lavorgna, R. Lamanna, Geopolymerization reaction to consolidate incoherent pozzolanic soil, J. Mater. Sci. 43 (2008) 865–873.
[20] J.G.S. van Jaarsveld, J.S.J. Van Deventer, G.C. Lukey, The effect of composition and temperature on the properties of fly ash- and kaolinite-based géopolymers, Chem. Eng. J. 89 (2002) 63–73.
[21] J. Temuujin, R.P. Williams, A. van Riessen, Effect of mechanical activation of fly ash on the properties of geopolymer cured at ambient temperature, J. Mater. Proc. Technol. 209 (2009) 5276–5280.
[22] V.F.F. Barbosa, K.J.D. MacKenzie, C. Thaumaturgo, Synthesis and characterisation of materials based on inorganic polymers of alumina and silica: sodium polysialate polymers, Int. J. Inorg. Mater. 2 (2000) 309–317.
[23] K.J.D. MacKenzie, Utilization of non-thermally activated clays in the production of geopolymers, in: J. Provis, J.S.J. van Deventer (Eds.), Geopolymers: Structure, Processing, Properties and Applications, Woodhead, Cambridge, 2009, pp. 294–314.
[24] D.R.M. Brew, K.J.D. MacKenzie, Geopolymer synthesis using silica fume and sodium aluminate, J. Mater. Sci. 42 (2007) 3990–3993.
[25] K. Komnitsas, D. Zaharaki, Geopolymerisation: a review and prospects for minerals industry, Miner. Eng. 20 (2007) 1261–1277.
[26] J.G.S. van Jaarsveld, J.S.J. van Deventer, G.C. Lukey, The characterization of source materials in fly ash-based geopolymers, Mater. Lett. 57 (2003) 1272–1280.
[27] K.J.D. MacKenzie, M.E. Smith, A. Wong, A multinuclear MAS NMR study of calcium-containing aluminosilicate inorganic polymers, J. Mater. Chem. 17 (2007) 5090–5096.
[28] J.L. Provis, Modelling the formation of geopolymers, PhD Thesis, University of Melbourne, Australia, 2006.
[29] D.S. Perera, J.D. Cashion, G.M. Blackford, Z. Zhang, E.R. Vance, Fe speciation in geopolymers with Si/Al molar ratio of 2, J. Eur. Ceram. Soc. 27 (2007) 2697–2703.
[30] J. Temuujin, A. van Riessen, K.J.D. MacKenzie, Preparation and characterisation of fly ash based geopolymer mortars, Constr. Build. Mater. 24 (2010) 1906–1910.
[31] P. Duxson, G.C. Lukey, J.S.J. van Deventer, Thermal evolution of metakaolin geopolymers. Part 1. Physical evolution, J. Non-Cryst. Sol. 352 (2006) 5541–5555.